DOI: 10.1002/chem.200600619

The Molecular Basis of Self-Assembly of Dendron–Rod–Coils into One-Dimensional Nanostructures

Eugene R. Zubarev,[a, b] Eli D. Sone,[a] and Samuel I. Stupp*[a]

Abstract: We describe here a comprehensive study of solution and solid-state properties of self-assembling triblock molecules composed of a hydrophilic dendron covalently linked to an aromatic rigid rod segment, which is in turn connected to a hydrophobic flexible coil. These dendron–rod–coil (DRC) molecules form well-defined supramolecular structures that possess a ribbonlike morphology as revealed by transmission-electron and atomic-force microscopy. In a large variety of aprotic solvents, the DRC ribbons create stable networks that form gels at concentrations as low as 0.2% by weight DRC. The gels are thermally irreversible and do not melt at elevated temperatures, indicating high stability as a result of strong noncovalent interactions among DRC molecules. NMR experiments show that the strong interactions leading to aggregation involve mainly the dendron and rodlike blocks, whereas oligoisoprene coil segments remain solvated after gelation. Small-angle X-ray scattering (SAXS) profiles of different DRC molecules demonstrate an excellent correlation between the degree-of-order in the solid-state and the stability of gels. Studies on two series of analogous molecules suggest that self-assembly is very sensitive to subtle structural changes and requires the presence of at least four hydroxyl groups in the dendron, two biphenyl units in the rod, and a coil segment with a size comparable to that of the rodlike block. A detailed analysis of crystal structures of model compounds revealed the formation of stable one-dimensional structures that involve two types of noncovalent interactions, aromatic π–π stacking and hydrogen bonding. Most importantly, the crystal structure of the rod–dendron compound shows that hydrogen bonding not only drives the formation of head-to-head cyclic structures, but also generates multiple linkages between them along the stacking direction. The cyclic structures are tetrameric in nature and stack into ribbonlike objects. We believe that DRC molecules utilize the same arrangement of hydrogen bonds and stacking of aromatic blocks observed in the crystals, explaining the exceptional stability of the nanostructures in extremely dilute solutions as well the thermal stability of the gels they form. This study provides mechanistic insights on self-assembly of triblock molecules, and unveils general strategies to create well-defined one-dimensional supramolecular objects.

Keywords: gels · self-assembly · structure elucidation · supramolecular chemistry

Introduction

Since Lehn[1] introduced the concept of "chemistry beyond the molecule" nearly 20 years ago, there has been great interest on the concept of programming molecules to create functional supramolecular assemblies.[2–5] Numerous examples of self-assembled structures reported to date include zero-,[6] one-,[7] and two-dimensional[8] assemblies based on hydrogen bonding,[9] metal–ligand coordinative bonds,[10] aromatic π–π stacking interactions,[11] and the hydrophobic effect.[12] Self-assembly has been used to create molecular capsules,[13] noncentrosymmetric clusters,[14] helical ribbons,[15] supramolecular polymers,[16] and double helical[17] and nanotubular[18] structures. In spite of the activity, the field of supramolecular science remains in its infancy.

Given that computational approaches are still of limited use in predicting self-assembly, once interesting systems are discovered it is important to carry out systematic studies on analogous compounds that mutate molecules to understand mechanistic details. In 2001 our laboratory reported on the

[a] Prof. E. R. Zubarev, Dr. E. D. Sone, Prof. S. I. Stupp
Department of Chemistry
Department of Materials Science and Engineering
Feinberg School of Medicine, Northwestern University
Evanston, IL 60208 (USA)
Fax: (+1) 847-491-3010
E-mail: s-stupp@northwestern.edu

[b] Prof. E. R. Zubarev
Current address: Department of Chemistry
Rice University, Houston, TX 77005 (USA)

self-assembling behavior of triblock molecules **1** referred to as dendron–rod–coils (DRCs).[19] These molecules form

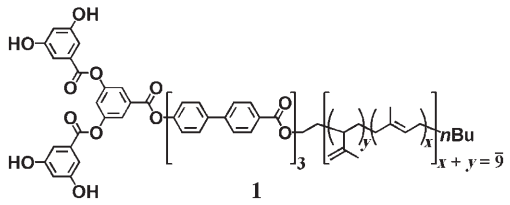

1

well-defined nanoribbons in nonpolar organic solvents. Such ribbons form highly robust gels,[20] organize nanocrystals,[21] and precisely template the growth of inorganic helical[22] and double helical[23] semiconductors. They can also scaffold the matrices of linear polymers and profoundly change their physical properties.[24] However, none of these advanced properties could be foreseen or predicted a priori as molecule **1** was indeed discovered by serendipity.

It was an intermediate compound in a multistep synthesis of high-generation DRCs,[25] and could have easily gone unnoticed were it not for its ability to form gels at exceedingly low concentrations. The molecular basis for self-assembly of these molecules is studied systematically in this paper, providing insight on strategies to create one-dimensional organic nanostructures.

Results and Discussion

The DRC molecule **1** can be regarded as an organogelator as it forms gels in at least 15 different solvents.[26] Complete immobilization of organic media occurs at concentration as low as 0.2 wt% when dichloromethane is used as a solvent (Figure 1). Examination of gels by optical microscopy revealed their first unusual characteristics. They were highly birefringent, although the content of dichloromethane was 99.8 wt%. The observed optical anisotropy was indicative of internal order generated by very small amounts of gelator. Immobilization of organic solvents generally implies the presence of a fibrous network, but most of the known organogels are optically isotropic.[27] Thus, the birefringence of DRC gels is not just the result of network formation, it indicates that a significant long-range order exists in the gel environment. This also suggests that the supramolecular fibers formed by DRC molecules may order solvent molecules that are in contact with them, thus generating the birefringence.

Another surprising feature of DRC gels is related to their thermal properties. While most of organogels[27] undergo reversible gel–liquid transformation at some specific temperature, the DRC gels do not melt. In fact, the gels form at elevated temperature (70–80 °C) and remain intact as the temperature continues to rise. If one heats in a sealed vessel a 0.5 wt% DRC gel in dichloromethane (b.p. = 39 °C at 1 atm) up to 100 °C, the vapor pressure of solvent will eventually destroy the glass container, but the gel will not transform into a liquid. Alternatively, if the gel is heated in an open vial, the solvent will gradually evaporate without any destruction of the gel, until only a thin film of solid DRC is left on the bottom. Therefore, DRC gels are *thermally irreversible*, unlike most of known organogels,[27] and that suggests an exceptional thermal stability of the solvated fibrous structures. When a small amount of gel is dispersed in excess dichloromethane, and cast on carbon substrates, long one-dimensional objects with aspect ratio as high as 1000 can be observed by transmission electron microscopy (TEM). Figure 2 shows the TEM image of an unstained DRC sample. The width of the strands is well-defined and measures approximately 10 nm. Considering the length of molecule **1** is 6.5 nm in its fully extended conformation, the structures should contain at least two DRC molecules in the cross-section.

The TEM image also suggests that the isolated one-dimensional structures are very stable given the dilute nature

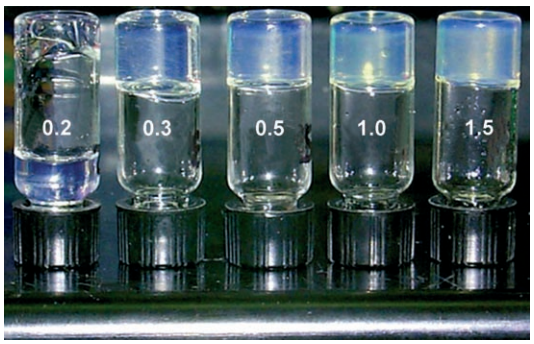

Figure 1. Photograph of self-supporting gels of DRC **1** in dichloromethane. The concentration of DRC is indicated in wt% on the vials.

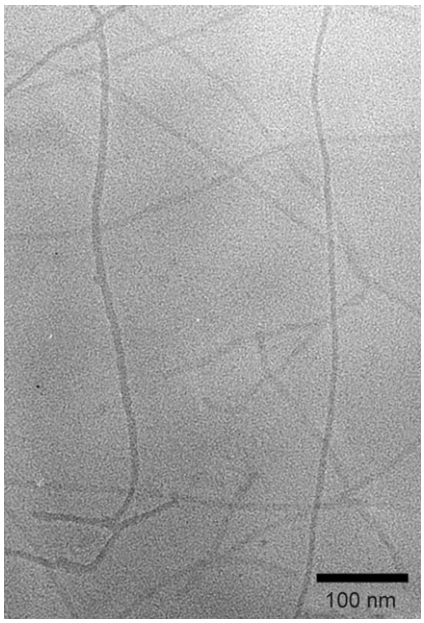

Figure 2. Bright-field TEM micrograph of unstained DRC nanoribbons formed in dichloromethane.

of the solution formed with a gelator concentration of 10^{-6} M. The ability of these supramolecular structures to retain their shape at such a low concentration indicates the presence of very strong internal forces, which may also be responsible for the high thermal stability of DRC supramolecular structures. Tilting experiments were used to confirm the ribbonlike morphology as reduction in the width of the strands from 10 to 8 nm (in projection) was observed upon a tilting of the sample stage of 30°. These findings were consistent with AFM experiments, which allowed us to accurately measure the thickness of the ribbons. Figure 3 shows

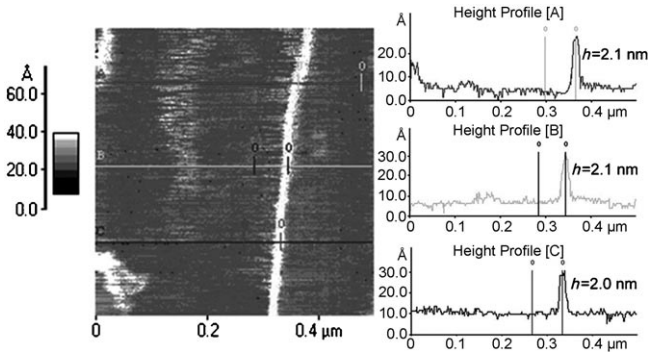

Figure 3. AFM image and height profiles of a nanoribbon formed by DRC molecules **1**. Height profiles along three arbitrary lines (A, B, and C) are shown on the right hand side.

the AFM image of an individual strand and the height profiles at three arbitrarily selected points along the one-dimensional structure. The height of the nanostructures was found to be approximately 2 nm and uniform along their length. Thus, the thickness of the strands is five times smaller than their width, and thus TEM and AFM demonstrate the ribbon morphology of the supramolecular aggregates. Because ribbons form in a nonpolar solvent (dichloromethane), it is reasonable to expect that DRC molecules adopt a head-to-head arrangement placing polar hydroxyl groups of the dendron blocks in the center of the ribbon. Such organization would minimize unfavorable contacts with the solvent molecules and may generate stable hydrogen bonds between OH groups. In addition, stacking of the preformed head-to-head hydrogen-bonded dimers along the axis of the ribbon would enable aromatic π–π interactions between the biphenyls of the rodlike midsections and the benzene rings of dendrons. The third block, oligoisoprene, would be located on the periphery and help ribbons retain their solubility in nonpolar solvents.

To corroborate this hypothesis we conducted NMR experiments and compared the signals generated by DRC molecules in their gels (using CD_2Cl_2 as the solvent), and as homogeneous solutions in THF (DRC **1** does not self-assemble in polar solvents such as THF or acetone). Figure 4 reveals a striking change in the rotational mobility of protons associated with aromatic segments upon gelation of the system. Aromatic peaks completely disappear in dichloromethane gels (bottom), but they remain very sharp and clearly re-

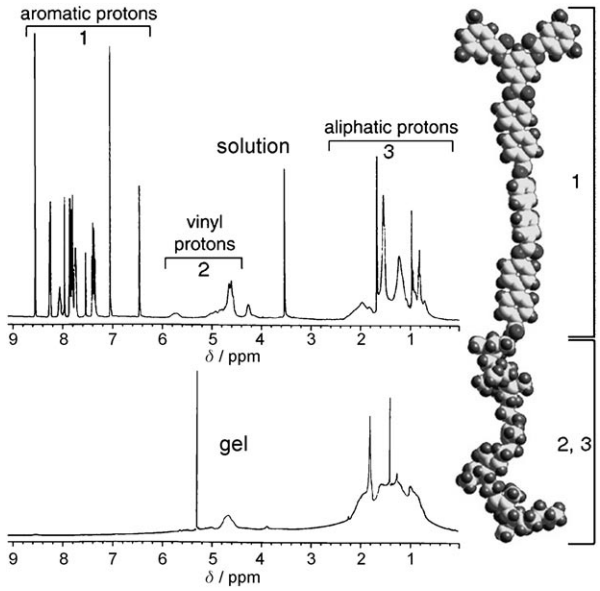

Figure 4. ^{1}H NMR spectra of a solution of DRC **1** in THF (top) and 1 wt % gel in methylene chloride (bottom). A molecular graphics representation of **1** is shown on the right.

solved in the NMR spectrum of solutions of **1** in THF (top). All three types of protons (aromatic, vinyl, and aliphatic) generate signals in THF, because molecules can freely rotate in the absence of aggregation. The signals that are not observed after gelation correspond to aromatic protons from both dendron and rod segments. The absence of these resonances indicates that a drastic decrease in motion has occurred, resulting in nonaveraging of magnetic anisotropies. The singlet at $\delta = 8.57$ ppm in THF spectrum corresponds to four hydroxyl groups in the dendron block. That signal is absent in the gel, which suggests possible hydrogen bonding as discussed previously. On the other hand, protons from oligoisoprene coil segments still generate intense but somewhat broadened peaks after gelation (Figure 4). Therefore, unlike the rod and dendron segments, oligoisoprene segments retain their rotational freedom in what appears to be a solvated self-assembled structure.

The fact that ribbons exist in an isolated state implies that their aggregation along edges and faces is not common. A strong tendency to aggregate would likely result in macrophase separation and precipitation. We noticed from the very beginning that a rod–coil precursor without the dendron block did not form gels and was insoluble in nonpolar solvents. Thus, the face-to-face packing of ribbons may be prevented by the presence of the bulky dendritic segments located at the center of the ribbon nanostructures. The dendrons can adopt a flat conformation so that the molecules could stack along the axis of the ribbon, but they would be much thicker than any other part of the ribbon. Similarly, edge-to-edge packing through oligoisoprene segments would be associated with a significant entropic loss, since the hydrophobic tails are highly solvated as shown by NMR spectroscopy. The ability of DRC ribbons to be stable in this iso-

lated state is in contrast to a large number of known organogelators, which typically form fibers that are not well-defined in terms of their cross-sectional dimension. In other words, conventional organogelators have only a limited preference for one-dimensional assembly. The molecular architecture of DRC molecules, on the other hand, strongly promotes one-dimensional self-assembly, yielding supramolecular polymers with well-defined ribbon architecture.

A logical question in this work is to ask what noncovalent interactions are responsible for triggering self-assembly and the high stability of DRC ribbons. NMR experiments suggest that both aromatic π–π stacking and hydrogen bonding are involved, but it cannot determine which interaction is more important. Initially, we believed that the presence of nine benzene rings in DRC molecule **1** and the well-known tendency of biphenyls to crystallize[14] should be sufficient for self-assembly even in the absence of OH groups. In an attempt to prove this idea we synthesized a series of analogous DRC molecules that differed only in the number of hydroxyl groups in the dendron segment (Table 1).

The first surprise came when we examined DRC **2**. It was highly soluble in dichloromethane and gelation did not occur even at concentrations approaching saturation. We therefore concluded that the presence of hydroxyl groups is necessary for self-assembly. Even two OH groups in DRC **3** did not lead to self-assembly of these molecules. This material was found to be insoluble in nonpolar solvents at room temperature, and formed clear isotropic solutions at elevated temperatures (Table 1). Numerous attempts to induce gelation by manipulating the cooling rate and the concentration were completely unsuccessful. This was a particularly puzzling observation, since the initially hypothesized formation of head-to-head dimers would not require more than two OH groups in the dendron to form such cyclic structures. Nonetheless, the analogous molecules DRC **4**, which contains six hydroxyl groups, self-assembled in dichloromethane and formed robust gels even at lower concentration than the original molecule DRC **1**. This series allowed us to conclude that at least four hydroxyl groups are required to drive self-assembly and that hydrogen bonding plays a critical role.

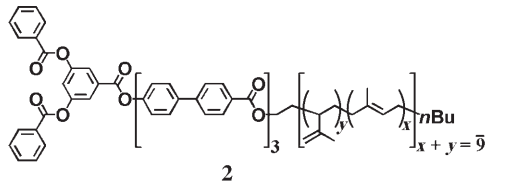

2

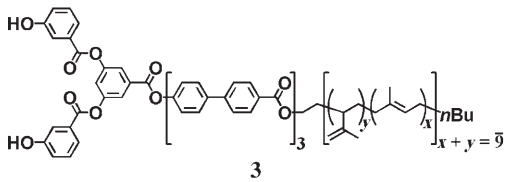

3

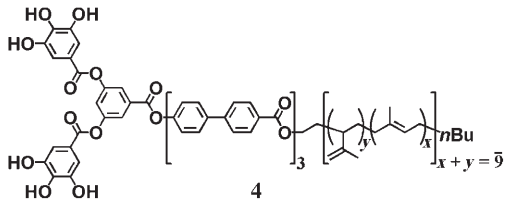

4

We investigated the solid-state organization in this series of molecules using small-angle X-ray techniques. Small-angle X-ray scattering (SAXS) was used to determine if there was any correlation between the order in the solid state and the ability of a given DRC analogue to self-assemble in solution. Figure 5 shows SAXS profiles collected from powder DRC samples. The original molecule **1** exhibits a significant degree of order as indicated by a very sharp peak at a *d* spacing of 94 Å (001) and the corresponding second order reflection at 47 Å (002). Since the fully extended length of DRC **1** is approximately 65 Å, we can conclude that in the solid state it forms a lamellar structure with bilayer packing involving partial interdigitation of molecules. The primary *d* spacing (9.4 nm) in the solid state is very close to the width of ribbons (10 nm) existing in solution as revealed by TEM. Thus, we expect that well-defined ribbon-like structures are present in the solid state as well. A very similar SAXS profile was obtained for molecule **4** ($d=$ 98 Å), which also self-assembles in solution. In contrast, the insoluble DRC **3** with two OH groups, generates a peak that is very different not only in terms of *d* spacing (82 Å), but also it is a broad peak in contrast to the sharp ones observed in DRC **1** and **4**. The 12 Å decrease in primary spacing in comparison with **1** is quite significant, since the length of all DRCs in this series is essentially the same (Table 1). In addition, the first-order diffraction peak is at least twice as broad, determined by measuring its width at half maximum of the first-order diffraction peak. These features indicate that the degree of crystalline order generated in the solid state of DRC **3** is considerably lower than in DRCs with four and six OH groups. These data also correlate very well with the fact that DRC **3**, unlike molecules **1** and **4**, does not form isolated self-assembled structures in solution. Fi-

Table 1. Molecules synthesized to probe hydrogen bonding versus self-assembly.

Compound	Number of OH groups	Extended length [Å][a]	*d* spacing [Å][b]	Observation
2	0	63	61	gelation not observed, isotropic solution at RT
3	2	65	82 major peak	gelation not observed, isotropic solution at elevated temperatures, insoluble at RT
1	4	65	94 (001), 47 (002)	blue-violet birefringent gel in nonpolar aprotic solvents
4	6	65	98 (001), 49 (002)	blue-violet birefringent gel in nonpolar aprotic solvents

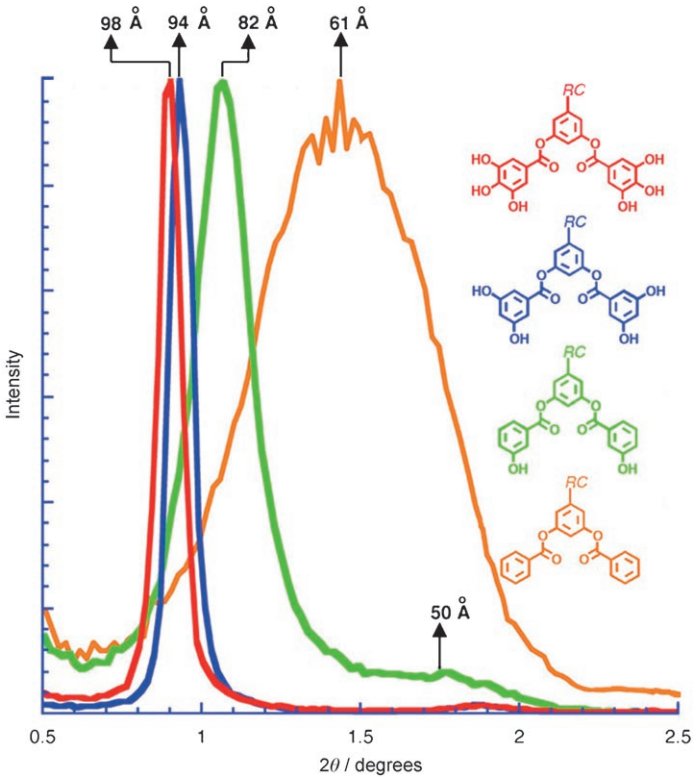

Figure 5. Solid-state SAXS profiles of analogous DRCs with variable number of hydroxyl groups. The chemical structure of molecules and the scattering plots are color-coded. RC stands for rod–coil portion, which is identical in all four structures.

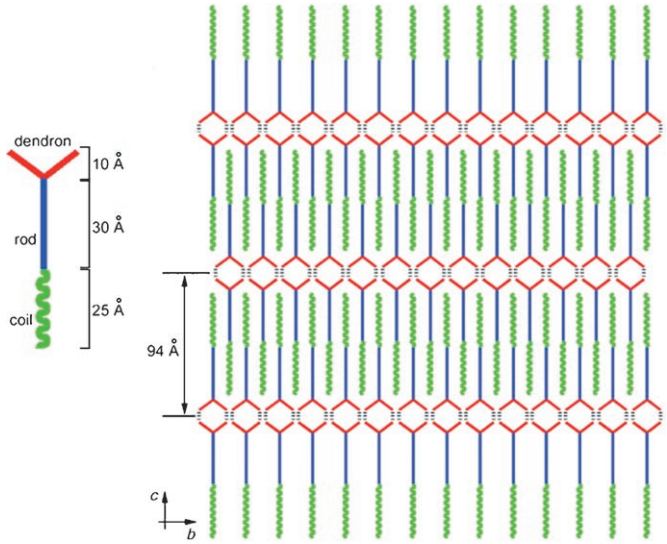

Figure 6. Proposed schematic representation of DRC **1** packing in the solid state. Each head-to-head dimer represents the cross-section of a ribbon oriented perpendicular to the plane of the figure.

nally, DRC **2**, which cannot form hydrogen bonds due to the absence of hydroxyl groups, produces an extremely broad peak centered at around 61 Å. This *d* spacing is already smaller than the fully extended length of the molecule (63 Å) and it suggests a monolayer packing in this DRC. It is likely that the head-to-head dimers do not form in this system as they would require the presence of hydroxyl groups. The extreme broadness of the peak is indicative of a low degree of crystalline order and inability of molecules **2** to generate long-range periodic structures. These findings were consistent with solution properties of DRC **2** as it readily dissolves in most organic solvents without any indication of self-assembly.

The exact packing of DRC molecules **1** in the solid state cannot be determined from SAXS, but it provides some important structural insights. Figure 6 shows a schematic representation of the molecular arrangement of DRC into a lamellar structure, which could be proposed on the basis of SAXS data and molecular modeling. Because the fully extended length of DRC is 65 Å, the observed primary spacing of 94 Å can be generated if there is a significant interdigitation involving both rods and coils as depicted in Figure 6. Each head-to-head dimer represents the cross-section of a ribbon oriented perpendicular to the plane of the graph. Within each layer ribbons may be packed in a face-to-face fashion along the *b* axis, whereas interdigitated edge-to-edge stacking of such layers along the *c* axis would produce the observed first-order diffraction peak (94 Å). Because the width of dendrons is significantly greater than that of rods or coils, the interdigitation would not cause steric repulsion and could effectively minimize the amount of free volume.

The combination of SAXS and TEM data also indicates that both face-to-face and edge-to-edge inter-ribbon interactions do not survive dissolution and must be much weaker than forces holding the molecules together within each individual ribbon. This once again points to the importance of hydrogen bonding in the self-assembly process, because multiple hydrogen bonds can easily form within each ribbon but may not readily form between them. The fact that DRC **3** with two OH groups does not produce ribbons suggests that in self-assembling DRCs **1** and **4**, hydroxyl groups may not only form dimers, but could also interconnect them along the axis of the ribbon. For example, two OH groups may be required to form a cyclic dimer, but two additional OH groups may participate in hydrogen bonding to adjacent neighbors. This way the intra-ribbon interactions would involve two types of noncovalent bonds, that is, aromatic π–π stacking and hydrogen bonding. In addition, the carbonyl groups of ester linkages can serve as hydrogen acceptors and their participation in stitching the dimers is also possible.

After examining the influence of the number of hydroxyl groups on self-assembly we considered the influence of π–π stacking interactions. For this purpose, a second series of molecules (**5**--**7**) was synthesized to probe the role of aromatic interactions in self-assembly (Table 2). In this series all the molecules have identical dendron segments with four hydroxyl groups and therefore retain the same capacity to form hydrogen bonds. However, the molecules differ in the number of biphenyl ester units forming their rodlike midsection. As shown in Table 2, molecules **5** (with one biphenyl–ester unit) do not gel organic solvents or produce the char-

Table 2. DRC molecules synthesized to probe aromatic interactions versus self-assembly.

Compound	Extended length [Å][a]	*d* spacing [Å][b]	Observation
5	45	62	viscous colorless solution in nonpolar solvents
6	55	78	blue-violet very weak gels in nonpolar solvents
1	65	94 (001), 47 (002)	blue-violet birefringent gels in nonpolar aprotic solvents
7	75	110 (001), 55 (002)	blue-violet birefringent gels in nonpolar and polar aprotic solvents

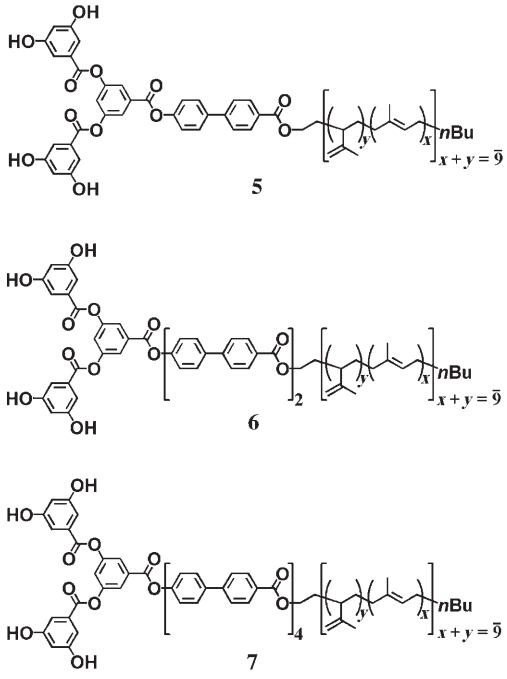

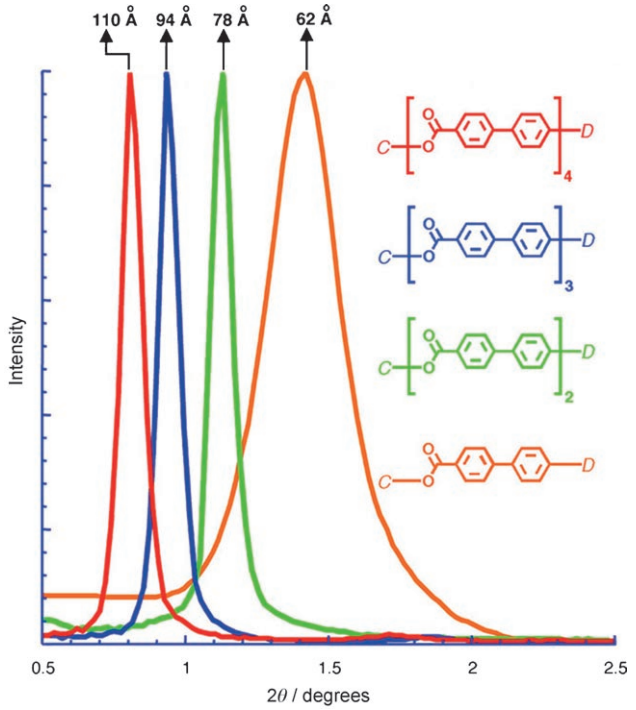

Figure 7. Solid-state SAXS profiles of analogous DRCs with variable number of biphenyl-ester repeat units. The chemical structure of molecules and the scattering plots are color-coded. C and D stand for coil (oligoisoprene) and dendron (4 OH groups), respectively.

acteristic blue-violet hue. In contrast, the addition of a second biphenyl ester unit in molecule **6** results in the formation of a gel, but one that is fairly unstable and weak, as it can easily rupture and lose its mechanical integrity upon shaking.

Self-assembly is further enhanced in molecules **7** containing four biphenyl groups, as indicated by the fact that gelation is now observed in a larger variety of solvents. For example, birefringent gels are obtained when **7** is dissolved in the monomeric polar solvents methyl methacrylate and *n*-butyl methacrylate, whereas **1** only forms isotropic solutions in these solvents. Thus, the results from this study show that hydrogen bonding alone may not be enough to trigger self-assembly and form stable supramolecular structures. At the same time, these findings may be related to changes in the mass fraction of the soluble block. For instance, in DRC **5**, the oligoisoprene segment accounts for 55% of the molecule's weight, whereas in DRC **7** its mass fraction drops to 37%. It appears that there is a very delicate balance involving not only the two different types of noncovalent interactions, but also the mass fractions of different blocks.

In analogy to the first series, we investigated the organization and the degree of crystalline order in the solid state. Figure 7 shows SAXS profiles obtained from DRCs with variable number of biphenyl units (**5**–**7**). The fully extended length of molecules in that series differs by approximately 10 Å (Table 2), and the observed 16 Å change in *d* spacing from one DRC to its nearest analogue is consistent with bilayered lamellar arrangement of all four molecules in this series. In addition, molecules **6** and **7** self-assemble in solution and their first-order diffraction peaks in the solid state are just as sharp as those of the original DRC **1** (Figure 7). In contrast, DRC **5** generates a much broader peak, although its primary *d* spacing (62 Å) is still consistent with a bilayered structure because its length is approximately 45 Å. These data once again demonstrate that there is a direct correlation between the ability of DRCs to self-assemble in solution and the degree of crystalline order in the solid state. Therefore, spontaneous formation of ribbonlike structural motifs through stacking of head-to-head dimers may be a universal property of these triblock molecules as long as they have at least four OH groups in the dendron and at least two biphenyl units in their rod segments.

In considering self-assembly of DRC molecules, it is important to take into consideration other molecular parameters, such as the mass fraction and the size of different blocks. Additional studies have shown that if the coil in

DRC becomes twice as long, gelation does not occur, whereas elimination of the coil segment renders the molecules completely insoluble in most organic solvents. Alternatively, the actual number of OH groups is only important when the generation of dendritic segment is equal to one. The DRCs with second-, third-, and fourth-generation dendrons do not self-assemble in spite of the fact that the number of hydroxyl groups in such molecules is 8, 16, and 32, respectively. This implies that the dendron should not be too bulky and should be able to adopt a nearly flat conformation to allow for dense one-dimensional stacking of molecules. High-generation dendrons tend to assume the entropically more favorable spherical conformation and that would hamper the self-assembling properties of the triblock structures. Conversely, if the generation of the dendritic segment is reduced to zero with dihydroxybenzoate moiety at its terminus, the molecules again lose their solubility. Finally, a drastic reduction in solubility and complete loss of self-assembling properties takes place if hydroxyl groups in DRC **1** are replaced by carboxyl groups, although they typically form much stronger hydrogen bonds. Thus, the self-assembly of DRCs is extremely sensitive to even subtle structural changes, and in our view it suggests a synergistic and very complex interplay of multiple enthalpic and entropic effects.

The aforementioned experimental data significantly clarified our understanding of structure–property relationship in DRCs and strongly advanced our knowledge comparing to what we knew about their gelation when we first discovered it by serendipity. However, interpretation of all these findings is largely based on the hypothesis that hydrogen-bonded cyclic dimers form in this system, and that they represent the main structural motif of the ribbons. Unfortunately, DRC **1** cannot be crystallized because it contains an oligoisoprene coil with random distribution of 1,4- and 3,4-addition units, and some limited polydispersity in the length of the coil segments. However, it is reasonable to believe that the crystal structure of model compounds, such as the analogous dendron or rod–dendron, molecules may have similar types and arrangements of hydrogen bonds. We started this investigation by preparing a dendron compound **DOH4**, which matched exactly the dendron block in the original molecule **1**. That compound was found to crystallize upon slow diffusion of *n*-pentane into a saturated solution of **DOH4** in ethyl acetate. Single crystals of sufficient quality for X-ray analysis were grown and the crystal structure was successfully solved.

Figure 8 shows nine unit cells viewed down the *a* axis of the crystal, which has $P2_1/n$ symmetry. Each monoclinic unit cell ($\beta = 94.23°$) is composed of four molecules of **DOH4** and measures $4.74 \times 19.33 \times 18.23$ Å. Multiple hydroxyl–hydroxyl and hydroxyl–carbonyl hydrogen bonds connect molecules into corrugated sheets that pack one atop the other. Most significantly, one can easily identify hydrogen-bonded cyclic dimers (color coded). Two OH···OH hydrogen bonds form each dimer, whereas two OH···O=C bonds in its center do not belong to a given cycle, but rather interconnect adjacent dimers along the [100] crystallographic direction, as will be discussed below. The two OH···OH hydrogen bonds that generate a dimer are very strong as the H···O distance measures 1.851 Å and the O–H···O angle is close to 166°. The third hydroxyl group of each molecule connects dimers along the vertical direction (*b* axis). At the same time, the fourth hydroxyl group participates in interdimer connections along the *c* axis as the dimers are linked through double OH···O=C hydrogen bonds (Figure 8). Interestingly, this same hydroxyl group is involved in the formation of the second hydrogen bond (OH···OH) stitching the dimers along the *b* axis, and therefore it simultaneously serves as a donor and acceptor of a proton (Figure 8). In essence, the (100) plane of the crystal is composed of horizontal rows of doubly hydrogen-bonded dimers. However, there are two different types of such rows because the orientation of dimers alternates along the [011] crystallographic direction. Overall, there are eight hydrogen bonds associated with

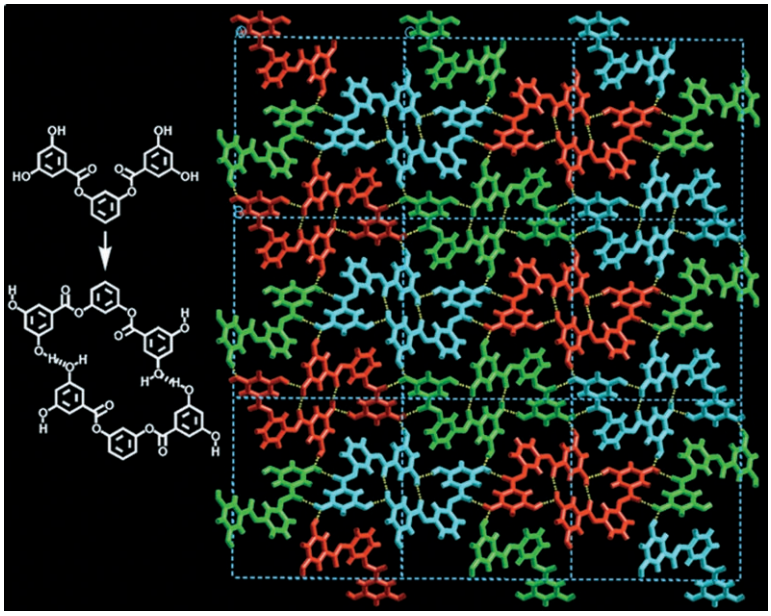

Figure 8. X-ray crystal structure of dendron compound **DOH4**. The image shows nine unit cells viewed along the [100] crystallographic direction. Hydrogen-bonded cyclic dimers are color-coded. Crystal data are given in the Experimental Section.

each molecule **DOH4**. The head-to-head dimers form by means of two OH···OH bonds, whereas additional 12 hydrogen bonds link a given dimer to its neighbors. Therefore, the crystal of **DOH4** represents a three-dimensional hydrogen-bonded network.

The presence of cyclic dimers in the crystal of dendron compound **DOH4** is undoubtedly the important feature that supports our original hypothesis. However, even more significant insight is revealed when stacking along the *a* axis of the crystal is considered (Figure 9). Dimers stack one atop

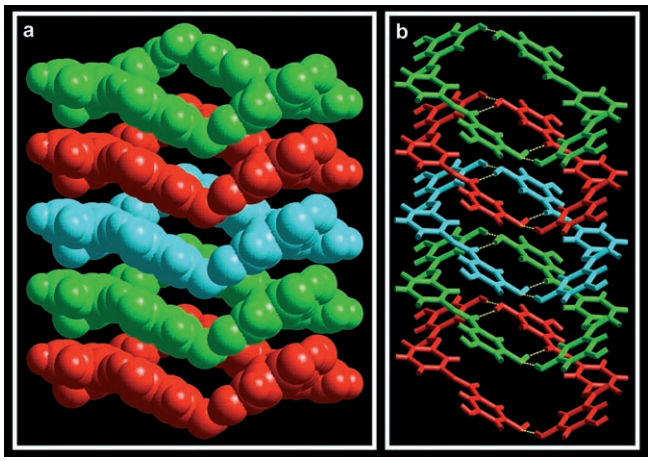

Figure 9. Side view of a stack of dimers taken directly from the crystal structure of dendron compound **DOH4** (each color represents a dimer pair). a) Space-filled rendition and b) stick model viewed perpendicular to the column direction. Two OH···OH hydrogen bonds form each cyclic dimer, whereas four OH···O=C hydrogen bonds connect each dimer to its adjacent neighbors along the stack axis that corresponds to the [100] direction.

the other and they are connected by multiple hydrogen bonds that essentially polymerize them along the stack axis. As mentioned previously, there are two intra-dimer hydrogen bonds (OH···OH, $d=1.85$ Å, $\theta=166°$), whereas four inter-dimer OH···O=C bonds ($d=1.84$ Å, $\theta=164°$) link each cycle to its upper and lower neighbors. The distance between the dimers is 4.74 Å, which indicates that they are also involved in aromatic face-to-face π–π stacking interactions. It must be emphasized that while many one-dimensional structures can be identified within this crystal, the stack of dimers along the *a* axis represents the only structural motif that involves two different types of noncovalent interactions simultaneously, that is, hydrogen bonding and π–π stacking interactions. Therefore, it should be more stable than any other one-dimensional ensemble in the crystal, such as rows of dimers along the *c* or *b* axes that are based on hydrogen bonding only. It is also interesting to note that the dimers adopt highly nonplanar conformation with the deviation from planarity of about 46°. This is the key structural feature which allows for the inter-dimer connections through hydrogen bonds. If the cycles had a flat conformation, the two central OH···O=C bonds would form internally. In that case each individual dimer would become more stable, but that would be a gain at the expense of stack's stability as there would be no hydrogen-bonded connections between the dimers. The crystal structure of the dendron compound **DOH4** reveals how the two different types of noncovalent interactions find a conformational compromise enabling their coexistence in the solid state. This also sheds light on how the central part of DRC ribbons may be organized, and why they have such high thermal and solution stability.

As discussed previously, the investigation of analogous series of DRCs clarified many aspects of their solution and solid-state properties, but it also generated one unsolved mystery. The DRC **3** with two OH groups was found not to self-assemble and that prompted us to synthesize and grow single crystals of a dendron compound with two OH groups (**DOH2**). Figure 10a shows the crystal structure of **DOH2** viewed along the [100] direction. The monoclinic unit cell ($3.94\times31.86\times12.60$ Å) is composed of four molecules that are hydrogen bonded. However, the crystal structure is distinctly different form that of compound **DOH4**, and we do not observe any head-to-head cyclic dimers. Instead, the molecules of **DOH2** form nearly linear dimers by means of two OH···O=C bonds ($d=1.94$ Å, $\theta=170°$). These two hydrogen bonds are internal for each linear dimer, and they are not used to connect adjacent neighbors along the *a* axis of the crystal, which is in stark contrast to **DOH4** dendron. The linear dimers are organized in a zigzag fashion, and create a two-dimensional corrugated layer. Another important feature of this crystal is the absence of OH···OH bonds as all the molecules are connected through only one type of hydrogen bond (OH···O=C). While one hydroxyl and one carbonyl attached to the same benzene ring of a molecule are involved in the formation of a linear dimer, the second hydroxyl and carbonyl groups create a branch as they link the dimer to its two neighbors along the *b* axis (Figure 10a). However, these connections are not between the dimers that belong to the same two-dimensional layer. The second hydroxyl group links to a dimer from the upper layer, whereas the second carbonyl group hydrogen bonds to a dimer from the lower layer ($d=1.98$ Å, $\theta=173°$). Hence, these groups create three-dimensional branching, and the linear dimers that compose a given layer do not form a two-dimensional hydrogen-bonded sheet as may appear in the projection (Figure 10a). As a result of this branching, the crystal is still a three-dimensional hydrogen-bonded network, but the total number of hydrogen bonds is significantly lower than that in **DOH4** crystals. Only four hydrogen bonds connect each linear dimer to its neighbors (Figure 10a), whereas each cyclic dimer in **DOH4** participates in twelve hydrogen bonds (Figure 10b).

A direct comparison between the crystal structures of dendron compounds (Figure 10) clearly demonstrates the influence of two extra hydroxyl groups on the overall packing and the type of interactions in the solid state. The most important difference is the presence of cyclic dimers in **DOH4** that are stitched by multiple hydrogen bonds, whereas in **DOH2** only linear dimers form and there are no hydrogen

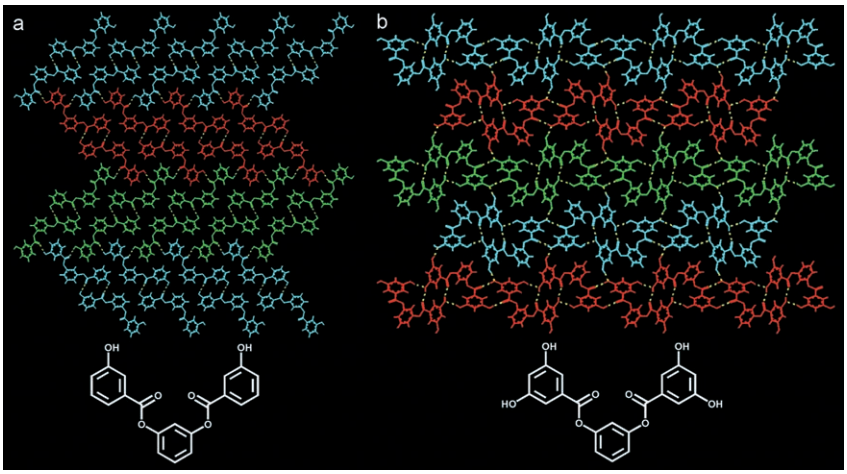

Figure 10. Comparison of the X-ray crystal structures of dendron compounds **DOH2** (a) and **DOH4** (b). The image shows a projection along the [100] direction. Only linear hydrogen-bonded dimers are present in the crystal of **DOH2** and they are arranged in a zigzag fashion along the *c* axis of the crystal. In contrast, cyclic dimers constitute the crystal of **DOH4** and multiple hydrogen bonds connect dimers along all three axes.

bonds connecting them along the *a* axis. Upon careful examination, however, one can also identify linear dimers in **DOH4**. For example, if we consider a row of green cyclic dimers in Figure 10b, the two molecules connecting the neighboring cycles actually form what appears to be a linear, although highly twisted, dimer similar to those present in **DOH2** crystals (Figure 10a). However, the two OH···O=C bonds that create such structures are once again internal links. They only connect the two molecules and do not participate in linking adjacent neighbors down the *a* axis. Thus, the stack of cyclic dimers is the most stable structural motif, since it involves both types of noncovalent interactions. Interestingly, the distance between the cyclic dimers in **DOH4** is significantly greater than that between the linear dimers in **DOH2**, as it decreases from 4.74 to 3.94 Å, respectively. This means that the π–π stacking interactions are stronger in **DOH2**, but this would still be negligible in comparison with four hydrogen bonds connecting the cyclic dimers in **DOH4**. On the basis of these data, we can conclude that the main reason for the absence of self-assembling properties in DRC **3** is directly related to the insufficient number of hydroxyl groups. While linear dimers can form in solutions of these molecules, the dendron segment with only two OH groups would not be able to generate inter-dimer hydrogen-bonded connections along the one-dimensional stack. Instead, hydroxyl and carbonyl groups that are not involved in the formation of such dimers may generate branches as observed in the crystal of **DOH2**. As a result, this would lead to a three-dimensional aggregation of dimers and subsequent precipitation. The fact that DRC **3** becomes soluble at elevated temperatures may imply the destruction of branching hydrogen bonds that are likely to form only randomly when a large rod-coil segment is present.

The crystal structures of dendritic molecules provide many important insights, but the far-reaching conclusions about the structure of DRC ribbons would still be premature at this point. The important question remains as to what effect the covalently attached rod–coils would have on the hydrogen-bonded structure. Unfortunately, our numerous attempts to crystallize model DRCs with aliphatic coils have not been successful. Crystallization of such molecules composed of three very different blocks is particularly problematic, if not impossible. First of all, one cannot find an organic solvent that would be simultaneously a bad solvent for the hydrophobic coil segment, the aromatic rod segment, and the hydrophilic dendron. These mutually exclusive requirements often resulted in the formation of gels, as opposed to high-quality crystals. For that reason, we initially eliminated the coil segment and started crystallizing rod–dendron compounds. However, the solubility of rod–dendrons with either three or two biphenyl groups is so low that even hot DMSO does not dissolve them to any appreciable extent. Thus, we were left with the rod–dendron compound containing one biphenyl unit. Although the molecules are fairly soluble in many organic solvents, its crystallization was a remarkably daunting task. It took 122 unsuccessful trials and consumed nearly nine months before conditions to grow X-ray quality crystals were finally found.

Figure 11 shows nine triclinic unit cells ($P\bar{1}$, 4.93×19.22×33.022 Å) of the crystal of rod-dendron compound viewed along the *a* axis. First of all, in this crystal we no longer observe cyclic dimers. Instead, each unit cell is represented by four molecules that form a hydrogen-bonded cyclic tetramer. The tetramers (color-coded) are connected along the *b* axis by means of multiple OH···O=C hydrogen bonds, and they stack one atop the other along the *a* axis with multiple inter-tetramer hydrogen bonds, as will be discussed below. In contrast, there are no hydrogen-bonded links between the tetramers along the *c* axis. Thus, the crystal is built of two-dimensional hydrogen-bonded sheets (parallel to the (001) plane) that are interdigitated along the *c* axis through biphenyl rods. The biphenyl units are arranged in a face-to-edge fashion ($d=5.62$ Å) along the *b* axis, and stack face-to-face along the *a* axis of the crystal ($d=4.93$ Å), which allows for the π–π stacking interactions. In addition, the crystal is a highly porous structure as tetramers form large channels (~15×7 Å) filled with solvent molecules (THF). Specifically, four THF molecules are associated with each unit cell. However, two of them are located in the cavity of a tetramer and they are hydrogen bonded to hydroxyl groups, whereas the two other molecules placed in the cavity between the tet-

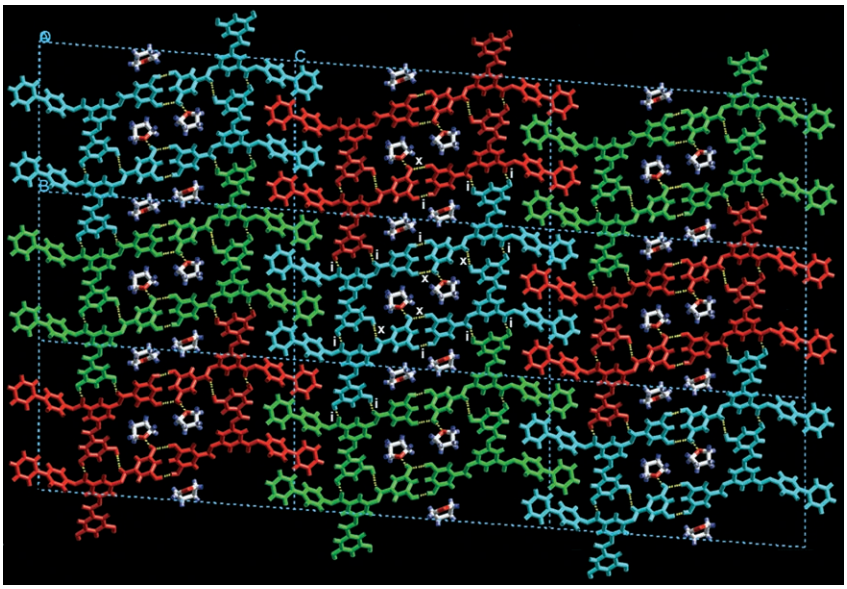

Figure 11. X-ray crystal structure of rod-dendron compound viewed along the [100] direction. The image shows nine unit cells represented by hydrogen-bonded cyclic tetramers (color-coded). Hydrogen bonds designated as **i** connect molecules within the (001) plane of the crystal. Yellow dashed lines designated **x** represent overlapped hydrogen bonds that connect tetramers along the *a* axis. Crystal data are given in the Experimental Section.

ramers have very different orientation and do not participate in hydrogen bonding.

The consideration of intra- and inter-tetramer hydrogen bonds and aromatic interactions allow us to identify the most stable one-dimensional motif in the crystal. Evidently, there are no continuous hydrogen-bonded rows along the *c* axis. On the other hand, the hydrogen-bonded stacks of tetramers along the *b* axis would not qualify either because the distance between the biphenyl units belonging to each individual stack is too large (13.52 Å). Thus, aromatic π–π interactions would not contribute to the stabilization of such one-dimensional structures, even though they have a ribbonlike morphology. The only direction in the crystal along which both types of noncovalent interactions hold molecules together is the [100] direction. If we consider a given tetramer (see blue tetramer, for example, in Figure 11) then multiple hydrogen bonds can be seen in two-dimensional projections, but not all of them participate in stitching the tetramers down the *a* axis. The yellow dashed lines designated **i** in Figure 11 represent hydrogen bonds that connect molecules within the (100) plane. There are 12 such bonds per tetramer. Four of them are responsible for the formation of a tetramer (intra-tetramer hydrogen bonds), whereas the other eight connect the tetramer to its neighbors along the *b* axis. The hydrogen bonds that link tetramers along the *a* axis (inter-tetramer bonds) are located in the interior of tetramer and they are marked **x** in Figure 11. However, each yellow dashed line designated **x** actually represents two overlapped hydrogen bonds. One of them connects a tetramer to its upper neighbor, and the other one links it to the lower neighbor. There are four sites of this type per tetramer and therefore eight hydrogen bonds connect a given tetramer to its adjacent neighbors along the *a* axis.

One may question whether the tetramers in Figure 11 formed by two molecules labeled with one color and two labeled with another color are the same as tetramers formed by four molecules of the same color. If a stack of tetramers with molecules of two different colors were isolated it would have only two **x** sites connecting the neighbors down the *a* axis (see a tetramer formed by two blue and two red molecules in Figure 11). These sites involve OH···OH bonds located on the upper and lower exterior sides of a tetramer with molecules of two different colors. Therefore, such a stack would have only four hydrogen bonds per tetramer to stitch adjacent neighbors, as opposed to eight hydrogen bonds connecting molecules of a tetramer with a single color along the *a* axis. This consideration shows that stacks of color-coded tetramers must be much more stable, if not the most stable, one-dimensional structures possessing a ribbonlike morphology.

In addition, one may consider linear dimers instead of cyclic tetramers. Their stack would also have both π–π stacking and hydrogen bonding along the *a* axis. However, such a stack of linear dimers has only one **x** site and therefore only two hydrogen bonds connect them down the *a* axis (one hydrogen bond per molecule). This is a twofold decrease in the number of hydrogen bonds in comparison with the tetrameric stacks (two hydrogen bonds per each molecule yielding a total of eight bonds). Finally, the thickness of DRC **1** ribbons determined experimentally by AFM (2 nm) nearly matches the thickness of the tetrameric stack (1.92 nm) from this crystal structure. Thus, the DRC ribbons are likely to be stacks of tetramers, as opposed to dimers that would be less stable and have a significantly smaller thickness.

It is interesting to consider the mechanism through which inter-tetramer linkages are formed along the stack axis. Figure 12 (top) shows a molecular graphics representation of an isolated tetramer taken directly from the crystal structure. Two OH···OH ($d=2.01$ Å, $\theta=176°$) and two OH···O=C ($d=1.90$ Å, $\theta=174°$) hydrogen bonds form the tetramer. Close examination reveals that there are two nearly parallel hydrogen bonds between the OH groups. These two H bonds point towards each other and appear as one bond in projection. In addition, there is one striking feature in this unit cell. It is composed of two pairs of very different conformers. While two molecules placed across one diagonal (1 and 4) have almost flat dendron segments, the other two

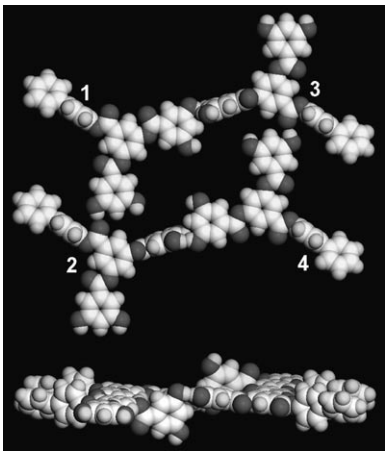

Figure 12. Top: Molecular graphics representation of a tetramer from the crystal structure of the rod–dendron compound. Bottom: Side view of the same tetramer rotated 90° along the *c* axis. The tetramer corresponds to one centrosymmetric unit cell of the crystal and consists of two pairs of different conformers.

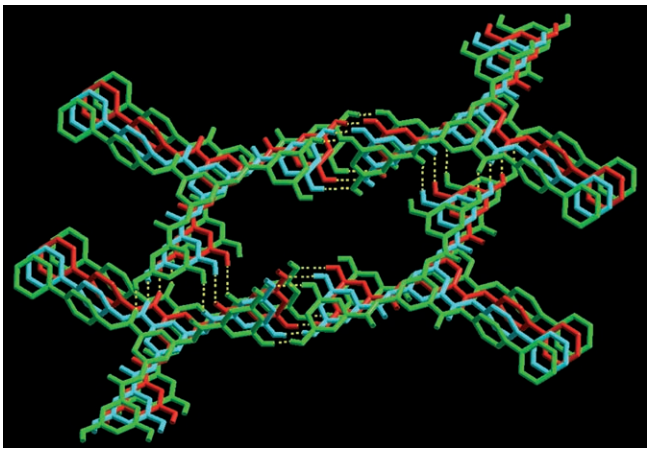

Figure 13. A top view of a stack of four tetramers taken from the crystal structure of rod–dendron compound. Two OH···OH and two OH···O=C hydrogen bonds (yellow dashed lines) connect four molecules to form a tetramer. Each tetramer is connected to its upper and lower neighbors via four OH···OH and four OH···O=C hydrogen bonds, which form two clockwise and two counterclockwise helical paths connecting adjacent tetramers along the *a* axis of the crystal.

molecules (2 and 3) adopt a conformation with nearly orthogonal orientation of one benzene ring with respect to the other two.

This is an important feature of this structure because it allows the formation of inter-tetramer connections. In fact, one ring points above and the other one points below the plane of tetramer (Figure 12, bottom). Each ring positions one hydroxyl and one carbonyl group towards an adjacent neighbor. Therefore, they generate four inter-tetramer hydrogen bonds. However, the total number of such bonds is eight as will be shown below.

Although the conformation of molecules 1 and 2 is different, they are related by pseudosymmetry (the same is true for molecules 3 and 4). Because the unit cell is centrosymmetric, one can say that molecules 1 and 3, and 2 and 4 are related by pseudo-twofold-screw symmetry (2_1) along the *a* axis. Another important element of the tetrameric unit cell is that four hydroxyl groups are pointing towards the interior of the tetramer (Figure 12, top). That suggests that the inner walls of the channel formed by tetramers are significantly more hydrophilic than the outer walls. This explains why the THF molecules located within the stack of tetramers are hydrogen bonded and those placed in the cavity between the tetramers are not. This may also be relevant to the properties of DRC ribbons, because they are formed in nonpolar solvents. Formation of tetrameric, as opposed to dimeric ribbons, could minimize unfavorable contacts between the hydroxyl groups and molecules of a nonpolar solvent.

When a stack of tetramers is extracted from the crystal and slightly tilted along the *c* axis, a remarkable interplay of both inter- and intra-tetramer hydrogen bonding can be observed. Figure 13 shows such stack of four color-coded adjacent neighbors. There are two sites involving OH···OH linkages that are located on the top and the bottom central part of the rectangular stack.

Two other sites based on OH···O=C hydrogen bonds are positioned across the diagonal. It can be seen that each tetramer forms four OH···OH and four OH···O=C bonds that link it to adjacent neighbors along the stack axis. Most interestingly, if we consider any of the four sites, a specific pattern of hydrogen bonding can be identified. For instance, in the central upper part an intra-tetramer OH···OH bond is followed by an inter-tetramer linkage, which in turn is followed by an intra-tetramer bond, and so on. Therefore, the hydrogen-bonded connection is following a helical path in a clockwise direction. On the other hand, hydrogen bonds in the central bottom part follow a counterclockwise helical path. In fact, all four sites have helical patterns as the diagonal sets of OH···O=C bonds also follow clockwise (lower left corner) and counterclockwise (upper right corner) paths. This is a particularly interesting observation, since the rod–dendron molecules are achiral. However, there might be a connection between this structural feature and the ability of DRC **1** ribbons to twist into well-defined helices in some solvents as observed in our previous studies.[19,22,23,24a]

In addition, a side view of the same stack of tetramers offers a better perspective on the geometry and directionality of hydrogen bonds piercing throughout the ribbonlike object (Figure 14). Nearly flat dendrons as well as peripheral biphenyl units are stacked in a face-to-face fashion with a 4.93 Å *d* spacing, and therefore they are involved in an aromatic π–π stacking interactions. All OH···OH hydrogen bonds are located in the center of the ribbonlike structure and they are almost parallel to a tetramer plane. If we consider a blue tetramer, two such horizontal hydrogen bonds connect it to the upper (green) neighbor and two other OH···OH bonds link it to the lower (red) tetramer. In contrast, OH···O=C bonds are nearly vertical as they directly

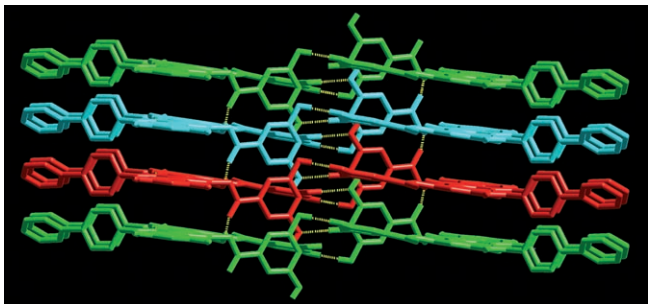

Figure 14. A side view of a stack of four tetramers taken from the crystal structure of the rod–dendron compound. Any given tetramer is connected by two hydroxyl–carbonyl hydrogen bonds to the upper (green) tetramer and two other hydroxyl–carbonyl hydrogen bonds to the lower (red) tetramer. These four hydrogen bonds are positioned nearly parallel to the axis of a stack (see vertical yellow dashed lines). Two central horizontal hydrogen bonds (OH···OH) connect the same blue tetramer to the upper (green) neighbor, and two other horizontal hydrogen bonds (OH···OH) connect it to the lower (red) neighbor.

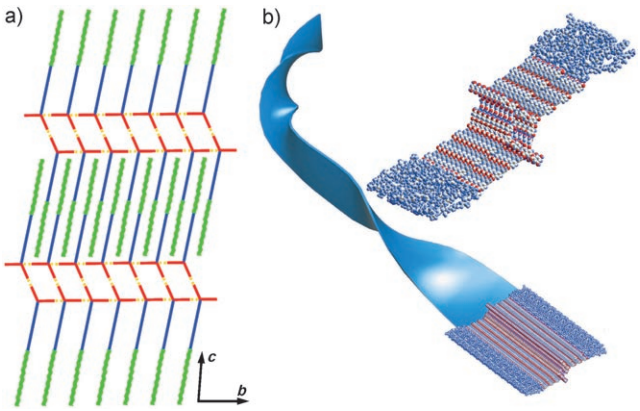

Figure 15. a) Proposed solid-state packing of DRC molecules based on SAXS profile of **1** and the crystal structure of the rod–dendron compound. b) Schematic and molecular graphics representation of the proposed tetrametic nanoribbon formed by DRC molecules **1**. The central spine of this ribbon is the tetrameric stack taken from the crystal structure of the rod–dendron compound. The rod–coil segments are covalently attached to the ribbon and are packed in a face-to-face arrangement (spaced 4.93 Å apart as defined by the crystal repeat).

connect adjacent neighbors along the axis of the stack. It is clear from this image that there are four such inter-tetramer connections per each tetrameric cycle. Benzene rings from nonplanar conformers play a key role in the formation of linkages between the tetramers without disrupting the π–π stacking interactions. Overall, there are four hydrogen bonds that form a tetramer and eight hydrogen bonds that connect it to adjacent neighbors. Although we do not know exactly the energy of these particular hydrogen bonds, we can still estimate that it would take ~40 kcal mol^{-1} to break the stack into individual tetramers if the energy of each hydrogen bond is about 5 kcal mol^{-1}. It would take an additional 20 kcal mol^{-1} to obtain isolated molecules. This energy is approaching the level of a typical covalent bond, and that may explain the fact that DRC ribbons do not melt and remain intact even at extremely low concentration (10^{-6} M).

On the basis of the crystallographic data, we can propose a more realistic model for the packing of DRC molecules **1** in the solid state and in solution. Figure 15a shows a possible arrangement of DRC molecules forming tetrameric cycles, as opposed to dimers (Figure 6). Because rods and coils cannot be involved in hydrogen bonding, it is reasonable to expect that a mere extension of the interdigitated part from one biphenyl unit to the rod–coil group would not disrupt the hydrogen-bonded central spine of the ribbonlike stack. The *d* spacing observed by SAXS (94 Å) would be consistent with fully interdigitated rod–coil segments. Upon dissolution of such solid, weak van der Waals contacts between the coils and rods would be broken first and would separate two-dimensional hydrogen-bonded sheets. As discussed previously, inter-tetramer contacts along the *b* axis are based only on hydrogen bonds and cannot involve π–π stacking interactions. Therefore, such face-to-face inter-ribbon contacts along the *b* axis are expected to break next, leading to isolated tetrameric ribbons that are based on both types of noncovalent interactions as depicted in Figure 15b. The thickness of such individual ribbons would be ~2 nm which is very close to the observed experimental value (Figure 3). Finally, two rows of benzene rings with two hydroxyl groups would be present of the surface of such ribbons. This feature may allow for random hydrogen-bonded contacts between the ribbons in solution and would help to form their networks leading to gelation in nonpolar organic solvents.

Conclusion

The triblock architecture and the interplay of two types of noncovalent interactions (hydrogen bonding and π–π stacking) are responsible for the ability of DRC molecules **1** to generate well-defined supramolecular polymers possessing a ribbonlike morphology. In this triblock architecture, the geometry of a low-generation dendritic segment capable of forming hydrogen bonds is key in the code for one-dimensional self-assembly in solution. However, the two other blocks, particularly the coil segment, are also necessary in conjunction with the dendron to drive one-dimensional aggregation. The hydrophobic oligoisoprene block is highly solvated as revealed by NMR spectroscopy and precludes edge-to-edge aggregation of the ribbons, whereas the presence of bulky dendrons in the central part of the ribbons resists their face-to-face packing. Hydroxyl groups of the dendron not only drive the formation of the cyclic head-to-head structures, but most importantly can stitch the one-dimensional object with multiple hydrogen bonds along its principal axis. Our studies demonstrate that the blueprint for robust self-assembly of one-dimensional organic nanostructures requires not only design of interactions among molecules but also the use of molecular shape to frustrate packing in the two other dimensions.

Experimental Section

Three model compounds **DOH2**, **DOH4**, and rod–dendron as well as the DRC molecules **1–7** were synthesized following the procedures described in detail in our previous publications.[19] Gels of DRC **1** were prepared by placing a solid DRC and dichloromethane into a capped vessel followed by heating the suspension to 70–80 °C. Complete dissolution of **1** resulted in the formation of a nonviscous clear solution, which rapidly (~10 s) turned into viscous solution with a blue-violet hue and further into a gel within 1–2 min at 70–80 °C. The vessel was cooled to room temperature, and the resulting gels were optically transparent and exhibited a blue-violet hue due to the Tyndall effect. Neither phase separation nor precipitation was observed in these systems, and the gels remained stable indefinitely. Temperature-induced melting of the DRC gels was never observed even when a sealed vessel was heated to 100 °C (61° above the boiling point of CH_2Cl_2), at which point the vapor pressure typically destroyed the container. The gels could only be disassembled by introducing polar solvents such as tetrahydrofuran (THF) or methanol, which could strongly compete for hydrogen bonding with carbonyl and hydroxyl groups of DRC **1**. The critical gelation point was found to be 0.2 wt% in CH_2Cl_2 (i.e., the lowest concentration at which the gel could sustain its own weight upon inversion of the container). The ^{1}H NMR spectra of the DRC molecular solution and the gel were obtained in [D_8]THF and CD_2Cl_2, respectively, using Varian U400 (400 MHz) spectrometer. Chemical shifts were expressed in parts per million (δ) using residual solvent protons as internal references.

Small-angle X-ray scattering (SAXS) experiments were carried out on a Siemens Anton Paar high-resolution small-angle camera equipped with a Hi-Star area detector and Bruker (Siemens) SAXS software mounted on an M18X-HF22 SRA rotating anode generator. Powder diffraction rings were integrated over 360° to yield the patterns and were calibrated by using a silver behenate standard (d = 58.376 Å). In most experiments the exposure time was 30 min. DRC powders used in SAXS experiments were prepared by casting a 1 wt% THF solution on glass substrate and subsequent annealing of the thin film (~100 microns) under nitrogen atmosphere at 120 °C for 2 h. The film was then scratched with a razor blade and the powder sample was packed into a cavity of standard polystyrene holder (3 mm in diameter and 2 mm in thickness).

Single-crystal X-ray scattering was used to determine the crystal structure of model compounds. The data were collected at 193 K on a Siemens SMART system equipped with a CCD detector using MoK_α radiation (λ = 0.71073 Å). The data were filtered to remove statistical outliers and the integration software (SAINT) was used to test for crystal decay as a bilinear function of X-ray exposure time and sin(θ). The structures were solved using SHELXTL by direct methods; correct atomic positions were deduced from an E map or by an unweighted difference Fourier synthesis. Non-hydrogen atoms were refined with anisotropic thermal coefficients. Successful convergence of the full-matrix least-squares refinement of F^2 was indicated by the maximum shift/error for the last cycle.

Crystals of dendron compound **DOH4** were grown by diffusion of *n*-pentane to a saturated solution of **DOH4** in ethyl acetate over a period of two days. A 0.05 × 0.25 × 0.35 mm single crystal was mounted on a thin glass fiber under oil (paratone-N, Exxon) and cooled immediately to 193 K. Crystal data for **DOH4**: $C_{20}H_{14}O_8$, M_r = 382.33, monoclinic, $P2_1/n$, a = 4.7397(5), b = 19.330(2), c = 18.235(2) Å, β = 94.230(2)°, V = 1670.3(5) Å^3, Z = 4. The structure was solved using SHELXTL V5.03 program and refined by using full-matrix least-squares on F_o^2, converging to $R1$ = 0.046 [2283 reflns; $F_o > 4\sigma(F_o)$], $wR2$ = 0.0912 (4010 reflns; all data).

Crystals of dendron compound **DOH2** were grown from a saturated ethyl acetate solution (~5 wt%) prepared at 60 °C and slowly cooled to room temperature. A 0.23 × 0.37 × 0.78 mm single crystal was mounted on a thin glass fiber under oil and cooled immediately to 193 K. Crystal data for **DOH2**: $C_{20}H_{14}O_6$, M_r = 366.35, monoclinic, $P2_1/n$, a = 3.9395(5), b = 31.8593(4), c = 12.5972(3) Å, β = 94.628(6)°, V = 1581.1(5) Å^3, Z = 4. The structure was solved using SHELXTL V5.03 program and refined using full-matrix least-squares on F_o^2, converging to $R1$ = 0.037 [1897 reflns; $F_o > 4\sigma(F_o)$], $wR2$ = 0.0788 (4325 reflns; all data).

Crystals of the rod–dendron compound were grown by diffusion of *n*-heptane to a 10 wt% solution in THF over a period of three days. A 0.08 × 0.15 × 0.40 mm single crystal was mounted on a thin glass fiber under oil and rapidly cooled to 193 K. Crystal data: $C_{33}H_{22}O_{10}$, M_r = 578.51, triclinic, $P\bar{1}$, a = 4.9341(5), b = 19.219(2), c = 33.022(3) Å, α = 85.805(2)°, β = 88.850(2)°, γ = 88.669(2)°, V = 3131.4(6) Å^3, Z = 4. The structure was solved using SHELXTL V5.03 program and refined using full-matrix least-squares on F_o^2, converging to $R1$ = 0.0928 [3305 reflns; $F_o > 4\sigma(F_o)$], $wR2$ = 0.3409 (10959 reflns; all data).

CCDC 616040 and CCDC 616041 contain the supplementary crystallographic data for this paper. These data can be obtained free of charge from The Cambridge Crystallographic Data Centre via www.ccdc.cam.ac.uk/data_request/cif.

Imaging of DRC **1** nanoribbons was carried out by atomic force microscopy (AFM). Samples were prepared by suspending a small portion of a 1 wt% gel in methylene chloride (typically 10 mg of gel in 2 mL CH_2Cl_2), and casting 1–2 droplets on graphite substrates. A Digital Instruments Multimode AFM and Nanoscope III controller were used to obtain height and phase contrast scans of dispersed nanoribbons. The AFM was operated in the tapping mode using 125 μm etched silicon probes with a tip radius ~10 nm. Surfaces were probed at several random locations with widely varying scan sizes from 0.2 to 20 μm. Typical forces were a few nanonewtons with scan rates of 0.5–1 Hz.

Acknowledgements

This work was supported by The Department of Energy (DE-FG02–00ER45810) and the U.S. Army Research Office MURI Grant (DAAG55–97–0126). Any opinions, findings, and conclusions or recommendations expressed in this publication are those of the authors and do not necessarily reflect the views of the DoE or US ARO. The authors are particularly thankful to Professor Jeffrey D. Hartgerink for very helpful experimental suggestions.

[1] a) J.-M. Lehn, *Science* **1985**, *227*, 849–856; b) J.-M. Lehn, *Angew. Chem.* **1990**, *102*, 1347–1362; *Angew. Chem. Int. Ed. Engl.* **1990**, *29*, 1304–1319; c) J.-M. Lehn, *Supramolecular Chemistry: Concepts and Perspectives*, VCH: Weinheim, **1995**.

[2] a) *Comprehensive Supramolecular Chemistry* (Eds.: J. L. Atwood, J. E. D. Davies, D. D. MacNicol, F. Vögtle, J.-M. Lehn), Pergamon, Oxford, **1996**; b) J. L. Atwood, G. W. Gokel, *Nature* **1991**, *354*, 354–355.

[3] a) G. M. Whitesides, J. P. Mathias, C. T. Seto, *Science* **1991**, *254*, 1312–1319; b) G. M. Whitesides, E. E. Simanek, J. P. Mathias, C. T. Seto, D. N. Chin, M. Mammen, D. M. Gordon, *Acc. Chem. Res.* **1995**, *28*, 37–44.

[4] a) M. C. T. Fyfe, J. F. Stoddart, *Acc. Chem. Res.* **1997**, *30*, 393–401; b) V. Balzani, A. Credi, F. M. Raymo, J. F. Stoddart, *Angew. Chem.* **2000**, *112*, 3486–3531; *Angew. Chem. Int. Ed.* **2000**, *39*, 3348–3391.

[5] a) J. Rebek, Jr., *Science* **1987**, *235*, 1478–1484; b) R. Wyler, J. de Mendoza, J. Rebek, Jr., *Angew. Chem.* **1993**, *105*, 1820–1821; *Angew. Chem. Int. Ed. Engl.* **1993**, *32*, 1699–1701; c) J. Rebek, Jr., *Acc. Chem. Res.* **1999**, *32*, 278–286.

[6] a) S. Leininger, B. Olenyuk, P. J. Stang, *Chem. Rev.* **2000**, *100*, 853–908; b) L. R. MacGillivray, J. L. Atwood, *Nature* **1997**, *389*, 469–472; c) R. S. Meissner, J. Rebek, Jr., J. de Mendoza, *Science* **1995**, *270*, 1485–1488; d) S. C. Zimmerman, F. W. Zeng, D. E. C. Reichert, S. V. Kolotuchin, *Science* **1996**, *271*, 1095–1098; e) L. J. Prins, J. Huskens, F. de Jong, P. Timmerman, D. N. Reinhoudt, *Nature* **1999**, *398*, 498–502; f) J. N. Cha, H. Birkedal, L. E. Euliss, M. H. Bartl, M. S. Wong, T. J. Deming, G. D. Stucky, *J. Am. Chem. Soc.* **2003**, *125*, 8285–8289; g) B. L. Frankamp, O. Uzun, F. Ilhan, A. K. Boal, V. M. Rotello, *J. Am. Chem. Soc.* **2002**, *124*, 892–893; h) Y. Zhou, M. Antonietti, *J. Am. Chem. Soc.* **2003**, *125*, 14960–14961; i) L. F.

Zhang, C. Bartels, Y. S. Yu, H. W. Shen, A. Eisenberg, *Phys. Rev. Lett.* **1997**, *79*, 5034–5037.

[7] a) H. Engelkamp, S. Middelbeek, R. J. M. Nolte, *Science* **1999**, *284*, 785–788; b) H. Fenniri, M. Packiarajan, K. L. Vidale, D. M. Sherman, K. Hallenga, K. V. Wood, J. G. Stowell, *J. Am. Chem. Soc.* **2001**, *123*, 3854–3855; c) L. Brunsveld, B. J. B. Folmer, E. W. Meijer, *MRS Bull.* **2000**, *25*, 49–53; d) E. A. Archer, N. T. Goldberg, V. Lynch, M. J. Krische, *J. Am. Chem. Soc.* **2000**, *122*, 5006–5007; e) Y.-Y. Won, H. T. Davis, F. S. Bates, *Science* **1999**, *283*, 960–963; f) J. D. Hartgerink, T. D. Clark, M. R. Ghadiri, *Chem. Eur. J.* **1998**, *4*, 1367–1372; g) J. D. Hartgerink, E. Beniash, S. I. Stupp, *Science* **2001**, *294*, 1684–1688.

[8] a) S. I. Stupp, S. Son, H. C. Lin, L. S. Li, *Science* **1993**, *259*, 59–63; b) C. D. Mao, W. Q. Sun, N. C. Seeman, *J. Am. Chem. Soc.* **1999**, *121*, 5437–5443; c) V. A. Russell, C. C. Evans, W. J. Li, M. D. Ward, *Science* **1997**, *276*, 575–579; d) E. Winfree, F. R. Liu, L. A. Wenzler, N. C. Seeman, *Nature* **1998**, *394*, 539–544; e) S. A. Bourne, J. J. Lu, A. Mondal, B. Moulton, M. J. Zaworotko, *Angew. Chem.* **2001**, *113*, 2169–2171; *Angew. Chem. Int. Ed.* **2001**, *40*, 2111–2113; f) H. Zepik, E. Shavit, M. Tang, T. R. Jensen, K. Kjaer, G. Bolbach, L. Leiserowitz, I. Weissbuch, M. Lahav, *Science* **2002**, *295*, 1266–1269; g) E. Mena-Osteritz, A. Meyer, B. M. W. Langeveld-Voss, R. A. J. Janssen, E. W. Meijer, P. Bauerle, *Angew. Chem.* **2000**, *112*, 2791–2796; *Angew. Chem. Int. Ed.* **2000**, *39*, 2679–2684; h) Y. Lin, H. Skaff, T. Emrick, A. D. Dinsmore, T. P. Russell, *Science* **2003**, *299*, 226–229; i) H. Spillmann, A. Dmitriev, N. Lin, P. Messina, J. V. Barth, K. Kern, *J. Am. Chem. Soc.* **2003**, *125*, 10725–10728.

[9] a) T. Martin, U. Obst, J. Rebek, Jr., *Science* **1998**, *281*, 1842–1845; b) L. J. Prins, F. de Jong, P. Timmerman, D. N. Reinhoudt, *Nature* **2000**, *408*, 181–184; c) J. H. K. K. Hirschberg, L. Brunsveld, A. Ramzi, J. A. J. M. Vekemans, R. P. Sijbesma, E. W. Meijer, *Nature* **2000**, *407*, 167–170; d) C. A. Mirkin, R. L. Letsinger, R. C. Mucic, J. J. Storhoff, *Nature*, **1996**, *382*, 607–609; e) A. K. Boal, F. Ilhan, J. E. DeRouchey, T. Thurn-Albrecht, T. P. Russell, V. M. Rotello, *Nature* **2000**, *404*, 746–748; f) H. von Berlepsch, C. Bottcher, A. Ouart, C. Burger, S. Dahne, S. Kirstein, *J. Phys. Chem. B* **2000**, *104*, 5255–5262.

[10] a) P. J. Stang, *Chem. Eur. J.* **1998**, *4*, 19–27; b) B. Olenyuk, J. A. Whiteford, A. Fechtenkotter, P. J. Stang, *Nature* **1999**, *398*, 796–799; c) N. C. Gianneschi, P. A. Bertin, S. T. Nguyen, C. A. Mirkin, *J. Am. Chem. Soc.* **2003**, *125*, 10508–10509; d) C. T. Chen, K. S. Suslick, *Coord. Chem. Rev.* **1993**, *128*, 293–322; e) P. J. Hagrman, D. Hagrman, J. Zubieta, *Angew. Chem.* **1999**, *111*, 2798–2848; *Angew. Chem. Int. Ed.* **1999**, *38*, 2638–2684.

[11] a) X. B. Zeng, G. Ungar, Y. S. Liu, V. Percec, S. E. Dulcey, J. K. Hobbs, *Nature* **2004**, *428*, 157–160; b) Z. H. Wang, V. Enkelmann, F. Negri, K. Mullen, *Angew. Chem.* **2004**, *116*, 2006–2009; *Angew. Chem. Int. Ed.* **2004**, *43*, 1972–1975; c) S. A. Jenekhe, X. L. Chen, *Science* **1998**, *279*, 1903–1907; d) S. A. Jenekhe, X. L. Chen, *Science* **1999**, *283*, 372–375; e) G. A. Breault, C. A. Hunter, P. C. Mayers, *J. Am. Chem. Soc.* **1998**, *120*, 3402–3410; f) E. F. Connor, L. K. Sundberg, H. C. Kim, J. J. Cornelissen, T. Magbitang, P. M. Rice, V. Y. Lee, C. J. Hawker, W. Volksen, J. L. Hedrick, R. D. Miller, *Angew. Chem.* **2003**, *115*, 3915–3918; *Angew. Chem. Int. Ed.* **2003**, *42*, 3785–3788; g) F. Cozzi, M. Cinquini, R. Annuziata, J. S. Siegel, *J. Am. Chem. Soc.* **1993**, *115*, 5330–5331.

[12] a) N. S. Cameron, M. K. Corbierre, A. Eisenberg, *Can. J. Chem.* **1999**, *77*, 1311–1326; b) Y. Y. Won, A. K. Brannan, H. T. Davis, F. S. Bates, *J. Phys. Chem. B* **2002**, *106*, 3354–3364; c) Q. G. Ma, E. E. Remsen, C. G. Clark, T. Kowalewski, K. L. Wooley, *Proc. Natl. Acad. Sci. USA* **2002**, *99*, 5058–5063; d) K. Velonia, A. E. Rowan, R. J. M. Nolte, *J. Am. Chem. Soc.* **2002**, *124*, 4224–4225; e) D. Voulgaris, C. Tsitsilianis, *Macromol. Chem. Phys.* **2001**, *202*, 3284–3292; f) J. Teng, E. R. Zubarev, *J. Am. Chem. Soc.* **2003**, *125*, 11840–11841; g) J. Xu, E. R. Zubarev, *Angew. Chem.* **2004**, *116*, 5607–5612; *Angew. Chem. Int. Ed.* **2004**, *43*, 5491–5496; h) H. A. Klok, J. F. Langenwalter, S. Lecommandoux, *Macromolecules* **2000**, *33*, 7819–7826; i) D. J. Pochan, Z. Y. Chen, H. G. Cui, K. Hales, K. Qi, K. L. Wooley, *Science* **2004**, *306*, 94–97; j) C. J. Hawker, K. L. Wooley, *Science* **2005**, *309*, 1200–1205.

[13] a) T. Heinz, D. M. Rudkevich, J. Rebek, Jr., *Nature* **1998**, *394*, 764–766; b) J. L. Atwood, L. J. Barbour, A. Jerga, *Chem. Commun.* **2001**, 2376–2377; c) R. G. Chapman, G. Olovsson, J. Trotter, J. C. Sherman, *J. Am. Chem. Soc.* **1998**, *120*, 6252–6260; d) N. Takeda, K. Umemoto, K. Yamaguchi, M. Fujita, *Nature* **1999**, *398*, 794–796; e) A. Arduini, L. Domiano, L. Ogliosi, A. Pochini, A. Secchi, R. Ungaro, *J. Org. Chem.* **1997**, *62*, 7866–7868; f) F. Felluga, P. Tecilla, L. Hillier, C. A. Hunter, G. Licini, P. Scrimin, *Chem. Commun.* **2000**, 1087–1088.

[14] a) S. I. Stupp, V. LeBonheur, K. Walker, L. S. Li, K. E. Huggins, M. Keser, A. Amstutz, *Science* **1997**, *276*, 384–389; b) E. R. Zubarev, M. U. Pralle, L. M. Li, S. I. Stupp, *Science* **1999**, *283*, 523–526.

[15] a) R. Oda, I. Huc, M. Schmutz, S. J. Candau, F. C. MacKintosh, *Nature* **1999**, *399*, 566–569; b) Y. V. Zastavker, N. Asherie, A. Lomakin, J. Pande, J. M. Donovan, J. M. Schnur, G. B. Benedek, *Proc. Natl. Acad. Sci. USA* **1999**, *96*, 7883–7887; c) J. H. Jung, G. John, M. Masuda, K. Yoshida, S. Shinkai, T. Shimizu, *Langmuir* **2001**, *17*, 7229–7232; d) W. M. Hwang, D. M. Marini, R. D. Kamm, S. Q. Zhang, *J. Chem. Phys.* **2003**, *118*, 389–397; e) A. Aggeli, I. A. Nyrkova, M. Bell, R. Harding, L. Carrick, T. C. B. McLeish, A. N. Semenov, N. Boden, *Proc. Natl. Acad. Sci. USA* **2001**, *98*, 11857–11862; f) J. Song, Q. Cheng, S. Kopta, R. C. Stevens, *J. Am. Chem. Soc.* **2001**, *123*, 3205–3213; g) B. W. Messmore, P. A. Sukerkar, S. I. Stupp, *J. Am. Chem. Soc.* **2005**, *127*, 7992–7993.

[16] a) P. R. Ashton, D. Philp, N. Spencer, J. F. Stoddart, *Makromol. Chem. Macromol. Symp.* **1992**, *54–55*, 441–464; b) V. Percec, J. Heck, G. Johannson, D. Tomazos, M. Kawasumi, *J. Macromol. Sci. Part A* **1994**, *31*, 1031–1070; c) R. P. Sijbesma, F. H. Beijer, L. Brunsveld, B. J. B. Folmer, J. H. K. K. Hirschberg, R. F. M. Lange, J. K. L. Lowe, E. W. Meijer, *Science* **1997**, *278*, 1601–1604; d) N. Yamaguchi, H. W. Gibson, *Angew. Chem.* **1999**, *111*, 195–199; *Angew. Chem. Int. Ed.* **1999**, *38*, 143–147; e) V. Berl, M. Schmutz, M. J. Krische, R. G. Khoury, J.-M. Lehn, *Chem. Eur. J.* **2002**, *8*, 1227–1244; f) J. van Gestel, P. van der Schoot, M. A. J. Michels, *J. Chem. Phys.* **2004**, *120*, 8253–8261; g) B. W. Messmore, J. F. Hulvat, E. D. Sone, S. I. Stupp, *J. Am. Chem. Soc.* **2004**, *126*, 14452–14458.

[17] a) T. W. Bell, H. Jousselin, *Nature* **1994**, *367*, 441–444; b) V. Berl, I. Huc, R. G. Khoury, M. J. Krische, J.-M. Lehn, *Nature* **2000**, *407*, 720–723; c) J. Y. Lu, V. Schauss, *Inorg. Chem. Commun.* **2003**, *6*, 1332–1334; d) R. Iwaura, K. Yoshida, M. Masuda, M. Ohnishi-Kameyama, M. Yoshida, T. Shimizu, *Angew. Chem.* **2003**, *115*, 1039; *Angew. Chem. Int. Ed.* **2003**, *42*, 1009; e) I. Azumaya, D. Uchida, T. Kato, A. Yokoyama, A. Tanatani, H. Takayanagi, T. Yokozawa, *Angew. Chem.* **2004**, *116*, 1384–1387; *Angew. Chem. Int. Ed.* **2004**, *43*, 1360–1363.

[18] a) M. R. Ghadiri, J. R. Granja, R. A. Milligan, D. E. Mcree, N. Khazanovich, *Nature* **1993**, *366*, 324–327; b) B. S. Thomas, C. R. Safinya, R. J. Plano, N. A. Clark, *Science* **1995**, *267*, 1635–1638; c) G. W. Orr, L. J. Barbour, J. L. Atwood, *Science* **1999**, *285*, 1049–1052; d) H. Fenniri, B. L. Deng, A. E. Ribbe, *J. Am. Chem. Soc.* **2002**, *124*, 11064–11072; e) P. Terech, A. de Geyer, B. Struth, Y. Talmon, *Adv. Mater.* **2002**, *14*, 495; f) S. Vauthey, S. Santoso, H. Y. Gong, N. Watson, S. G. Zhang, *Proc. Natl. Acad. Sci. USA* **2002**, *99*, 5355–5360; g) K. S. Kim, S. B. Suh, J. C. Kim, B. H. Hong, E. C. Lee, S. Yun, P. Tarakeshwar, J. Y. Lee, Y. Kim, H. Ihm, H. G. Kim, J. W. Lee, J. K. Kim, H. M. Lee, D. Kim, C. Z. Cui, S. J. Youn, H. Y. Chung, H. S. Choi, C. W. Lee, S. J. Cho, S. Jeong, J. H. Cho, *J. Am. Chem. Soc.* **2002**, *124*, 14268–14279.

[19] E. R. Zubarev, M. U. Pralle, E. D. Sone, S. I. Stupp, *J. Am. Chem. Soc.* **2001** *123*, 4105–4106.

[20] J. D. Hartgerink, E. R. Zubarev, S. I. Stupp, *Curr. Opin. Solid State Mater. Sci.* **2001**, *5*, 355–361.

[21] L. M. Li, E. Beniash, E. R. Zubarev, W. Xiang, B. M. Rabatic, G. Zhang, S. I. Stupp, *Nat. Mater.* **2003**, *2*, 689–694.

[22] E. D. Sone, E. R. Zubarev, S. I. Stupp, *Angew. Chem.* **2002**, *114*, 1781–1785; *Angew. Chem. Int. Ed.* **2002**, *41*, 1705–1709.

[23] E. D. Sone, E. R. Zubarev, S. I. Stupp, *Small* **2005**, *1*, 694–697.

[24] a) E. R. Zubarev, M. U. Pralle, E. D. Sone, S. I. Stupp, *Adv. Mater.* **2002**, *14*, 198–203; b) J. C. Stendahl, L. M. Li, E. R. Zubarev, Y. R. Chen, S. I. Stupp, *Adv. Mater.* **2002**, *14*, 1540–1543; c) J. C. Stendahl, E. R. Zubarev, M. S. Arnold, M. C. Hersam, H. J. Sue, S. I. Stupp, *Adv. Funct. Mater.* **2005**, *15*, 487–493.

[25] E. R. Zubarev, S. I. Stupp, *J. Am. Chem. Soc.* **2002**, *124*, 5762–5773.

[26] Formation of gels was observed in the following organic solvents: dichloromethane, dibromomethane, diiodomethane, chloroform, bromoform, benzene, chlorobenzene, 1,3-dichlorobenzene, methanol, toluene, styrene, α-methylstyrene, ethyl methacrylate, 2-ethylhexyl methacrylate, and hexyl methacrylate.

[27] a) P. Terech, R. G. Weiss, *Chem. Rev.* **1997**, *97*, 3133–3159, and references therein; b) P. Terech R. G. Weiss, in *Surface Characterization Methods* (Ed.: A. J. Milling), Marcel Dekker, New York, **1999**; c) E. Ostuni, P. Kamarks, R. G. Weiss, *Angew. Chem. Int. Ed. Engl.* **1996**, *35*, 1324–1326; d) K. Murata, M. Aoki, T. Suzuki, T. Harada, H. Kawabata, T. Komori, F. Ohseto, K. Ueda, S. Shinkai, *J. Am. Chem. Soc.* **1994**, *116*, 6664–6676; e) M. Loos, J. Esch, I. Stokroos, R. M. Kellogg, B. L. Feringa, *J. Am. Chem. Soc.* **1997**, *119*, 12675–12676; f) J. H. Van Esch, B. L. Feringa, *Angew. Chem.* **2000**, *113*, 2351–2354; *Angew. Chem. Int. Ed.* **2000**, *39*, 2263–2266; g) S. Ahmed, X. Sallenave, F. Fages, G. M. Gundert, W. M. Muller, U. Muller, F. Vogtle, J. L. Pozzo, *Langmuir* **2002**, *18*, 7096–7101.

Received: May 2, 2006
Published online: August 7, 2006

